www.nature.com/aps

Acta Pharmacologica Sinica

ARTICLE

# Luteolin alleviates cognitive impairment in Alzheimer's disease mouse model via inhibiting endoplasmic reticulum stress-dependent neuroinflammation

Jie-jian Kou[1], Jun-zhuo Shi[1], Yang-yang He[1], Jiao-jiao Hao[1], Hai-yu Zhang[1], Dong-mei Luo[1], Jun-ke Song[2,3], Yi Yan[4,5], Xin-mei Xie[1], Guan-hua Du[2,3] and Xiao-bin Pang[1]

Luteolin is a flavonoid in a variety of fruits, vegetables, and herbs, which has shown anti-inflammatory, antioxidant, and anti-cancer neuroprotective activities. In this study, we investigated the potential beneficial effects of luteolin on memory deficits and neuroinflammation in a triple-transgenic mouse model of Alzheimer's disease (AD) (3 × Tg-AD). The mice were treated with luteolin (20, 40 mg · kg$^{-1}$ · d$^{-1}$, ip) for 3 weeks. We showed that luteolin treatment dose-dependently improved spatial learning, ameliorated memory deficits in 3 × Tg-AD mice, accompanied by inhibiting astrocyte overactivation (GFAP) and neuroinflammation (TNF-α, IL-1β, IL-6, NO, COX-2, and iNOS protein), and decreasing the expression of endoplasmic reticulum (ER) stress markers GRP78 and IRE1α in brain tissues. In rat C6 glioma cells, treatment with luteolin (1, 10 μM) dose-dependently inhibited LPS-induced cell proliferation, excessive release of inflammatory cytokines, and increase of ER stress marker GRP78. In conclusion, luteolin is an effective agent in the treatment of learning and memory deficits in 3 × Tg-AD mice, which may be attributable to the inhibition of ER stress in astrocytes and subsequent neuroinflammation. These results provide the experimental basis for further research and development of luteolin as a therapeutic agent for AD.

**Keywords:** Alzheimer's disease; luteolin; neuroinflammation; endoplasmic reticulum stress; astrocyte; 3 × Tg-AD mice; C6 cells

*Acta Pharmacologica Sinica* (2022) 43:840–849; https://doi.org/10.1038/s41401-021-00702-8

## INTRODUCTION

Alzheimer's disease (AD) is a neurological disorder characterized by deep memory loss and progressive dementia [1, 2]. It is the most common cause of dementia in the elderly (50%–70% of all dementias). More than 50 million patients worldwide are affected by AD, and this number is expected to double by 2050 [3]. As of today, the etiology of AD is still unknown and the treatment is far from satisfactory. Hence, a novel therapeutic strategy targeting pathological mechanisms underlying AD is of great necessity and value worldwide.

In addition to amyloid plaques (APs) formed by beta-amyloid protein (Aβ) [4] and neurofibrillary tangles (NFTs) [5], neuroinflammation and neuronal degeneration are the main pathological features of AD [6, 7]. Although APs and NFTs are considered to be the main causes of neuronal death in AD, it is obvious that the local chronic inflammatory response mediated by glial cells not only acts as a new bystander to APs and NFTs [8, 9] but is also involved in the pathogenesis as plaques and tangles.

Activation of glial cells and overexpression of inflammatory cytokines are manifested as early inflammatory responses in AD [10, 11]. Astrocytes are important glial cells in the central nervous system (CNS). They participate in a variety of physiological activities with numerous receptors on the cell surface and ion channels and affect the living environment of surrounding cells [12]. Under pathological conditions, these overactivated astrocytes promote the occurrence of a toxic microenvironment around neurons [13]. Therefore, astrocytes have drawn great attention from many brain pathology and treatment studies due to their special functional properties.

Persistent endoplasmic reticulum (ER) stress is considered to be the driver of many chronic diseases. The cellular response to ER stress is initiated with the induction of the unfolded protein response (UPR) [14]. In neurodegenerative disease, the accumulation of misfolded proteins in neurons and the accompanying ER stress can lead to neuronal dysfunction [15]. In addition, ER stress response of surrounding glial cells may cause abnormal inflammatory signals and promote disease progression. Numerous studies have reported upregulation of UPR was observed in brain samples from patients with AD [16]. Some have suggested that ER stress participated in the neurodegeneration by inducing the

[1]School of Pharmacy, Henan University, Kaifeng 475004, China; [2]State Key Laboratory of Bioactive Substances and Functions of Natural Medicines, Institute of Materia Medica, Chinese Academy of Medical Science and Peking Union Medical College, Beijing 100050, China; [3]Beijing Key Laboratory of Drug Target Identification and Drug Screening, National Center for Pharmaceutical Screening, Institute of Materia Medica, Chinese Academy of Medical Science and Peking Union Medical College, Beijing 100050, China; [4]Institute for Cardiovascular Prevention (IPEK), Ludwig-Maximilians-University Munich, Munich 80336, Germany and [5]DZHK (German Centre for Cardiovascular Research), Partner Site Munich Heart Alliance, Munich 80336, Germany
Correspondence: Xin-mei Xie (xxm@vip.henu.edu.cn) or Guan-hua Du (dugh@imm.ac.cn) or Xiao-bin Pang (pxb@vip.henu.edu.cn)
These authors contributed equally: Jie-jian Kou, Jun-zhuo Shi, Yang-yang He

Received: 3 December 2020 Accepted: 17 May 2021
Published online: 15 July 2021

accumulation of Aβ in AD [17], however, there are still gaps in understanding the specific mechanisms of ER stress-mediated neuroinflammation.

Luteolin (3′,4′,5,7-tetrahydroxy flavones) is a flavonoid widely found in plants (molecular structure is shown in Supplementary Fig. S1a). It is mainly distributed in various fruits, vegetables, and herbs, such as honeysuckle and Perilla, etc. It has anti-inflammatory, antioxidant, and neuroprotective effects [18, 19], but whether it affects the ER stress of AD disease remains to be elucidated.

In this study, we interrogated whether luteolin had therapeutic potential in AD, and explored whether the protective role of luteolin in nervous system function was due to the inhibition of ER stress-mediated neuroinflammation in astrocytes.

## MATERIALS AND METHODS

### Chemicals and reagents

Luteolin (purity ≥ 98.0%) was obtained from Sigma Technology (Danvers, USA). Nissl staining solution was purchased from Beyotime Biotechnology Co., Ltd. (Nanjing, China). TNF-α, IL-1β, and IL-6 ENzyme-linked Immunosorbent assay (ELISA) kits were provided by Elabscience Biotechnology Co., Ltd. (Wuhan, China). DAPI, Triton X-100, mammalian cell lysis reagent were purchased from Solarbio Science & Technology Co Ltd. (Beijing, China). Antibodies were purchased and used at the indicated dilutions for Western blots and immunostaining including: mouse anti-glial fibrillary acidic protein (GFAP), rabbit anti-COX-2, rabbit anti-iNOS, rabbit anti-NF-κBp65, rabbit anti-GRP78, rabbit anti-IRE1α, FITC-goat anti-mouse IgG (H + L) 488, and FITC-goat anti-rabbit IgG (H + L) 594 all from Abcam (Cell Signaling, Boston, MA, USA), and rabbit anti-β-actin, rabbit anti-IgG or mouse anti-IgG obtained from Proteintech Group, Inc. (Wuhan, China).

### Animals

3 × Tg-AD mice were obtained from the Chinese Academy of Military Medical Sciences. Wildtype (WT, C57BL/6J) mice were purchased from Sibeifu (Beijing) Biotechnology Co., Ltd. (Beijing, China). The animals were bred in-house to generate experimental animal cohorts. Male and female transgenic (Tg) or wildtype (WT) mice and littermate controls aged 8 months were used in all studies.

Oddo et al. generated a triple-transgenic model (3 × Tg-AD) harboring PS1 (M146V), APP (Swe), and tau (P301L) transgenes. Rather than crossing independent lines, they microinjected two transgenes into single-cell embryos from homozygous PS1 (M146V) knockin mice, generating mice with the same genetic background. 3 × Tg-AD mice progressively develop plaques and tangles. They provided a valuable model for evaluating potential AD therapeutics as the impact on both lesions can be assessed [20]. The genotype of 3 × Tg-AD mice was stable. We identified the genotype of the bred mice and proved that they were homozygous (data shown in Supplementary Fig. S3).

Animals were housed in a facility under 12-h light and dark cycle and had access to food and water ad libitum. All protocols used in animal experiments were in accord with the Guidelines for the Care and Use of Laboratory Animals (Ministry of Science and Technology of China). All experiments involving mice were approved by the Ethics and Animal Care Committee of Henan University.

### Experimental design

C57BL/6J mice and 3 × Tg-AD mice were divided into the following four groups: WT-Con, 3 × Tg-AD, 3 × Tg + Low (Luteolin 20 mg/kg), and 3 × Tg + High (Luteolin 40 mg/kg). Luteolin was dissolved in <1% DMSO and mice were injected intraperitoneally once a day for 3 weeks [21]. After 3 weeks of continuous administration, the navigation test was carried out for five consecutive days, followed by a probe test 24 h post the navigation test.

### Morris water maze

The mouse was placed in different starting positions in a circular pool (120 cm in diameter and 40 cm in height) that was filled with water (21–22 °C, made opaque by adding non-toxic white paint). A platform (diameter 8 cm) was hidden in a quarter of the pool 2 cm below the surface of the water, and there is a camera attached to the top of the pool. Special markings were installed in fixed positions on a screen around the pool. Mice were trained to find the hidden platforms by using distant visual cues within 90 s. If the animal was unable to find the platform within 90 s, it was guided to the platform and requested to stay there for 20 s.

The two acquisition trials were performed on mice per day during five consecutive days and each animal had three random starting points. The swimming pattern of each mouse was monitored and recorded using the ZS-001 system (Beijing, China) for the 90s.

A probe trial was conducted 24 h after the acquisition trial to test memory consolidation. During the experiment, the platform was removed from the pool, and the mice were allowed to swim freely. The time each mouse spent in the target area and the times it passed through the platforms were recorded for spatial-memory evaluation.

### Nissl's staining

The brain tissue was fixed in 4% paraformaldehyde for 48 h, then dehydrated with gradient alcohol and embedded with paraffin. In total, 5 μm sliced sections (by Leica RM2235, Germany) were deparaffinized following dimethyl benzene dewaxing, 100% (I, II), 80%, 70% alcohol every 5 min. Afterward tissue sections were stained with Nissl solution for 8 min, rinsed in ultrapure water, dehydrated in 100% (I, II) alcohol for 2 min each, cleared in xylene for 3 min, and mounted. All the sections were photographed in the microscope [22].

### Thioflavin S-staining

The brain tissue was removed from the skull and soaked in a 30% sucrose solution for 48 h and then be sectioned at 10 μm on a cryostat microtome (Leica CM1950, Germany). The brain sections were treated with 0.3% potassium permanganate solution for 5 min, 1% oxalic acid solution for 5 min, 1% sodium borohydride solution for 5 min, and PBS wash twice. Then 5 μg/mL PI solution was added to the tissue for 15 min, followed by 0.5% sulfur flavin S solution staining for another 15 min. Sections were then dehydrated with alcohol (70%, 80%, 90%, and 100% alcohol) for 2 min and sealed with an anti-fluorescence attenuation sealing tablet (Solarbio, Beijing, China). Staining sections were observed and photographed under a fluorescence microscope, and four mice in each group were stained.

### Immunohistochemical staining

Paraffin sections (5 μm) were blocked with 5% BSA and 0.3% triton X-100 in phosphate-buffered saline (PBS) at room temperature for 1 h, followed by antigen repair with citric acid buffer. The sections were then incubated with primary antibodies at 4 °C overnight, followed by specific secondary antibodies incubation for 30 min the second day. DAB was used for color development and hematoxylin for nuclear staining. The immunopositive cells were stained brown. The positive expression of the specific protein was observed under an inverted microscope. Immunohistochemical images were analyzed using Image J.2.0 (National Institutes of Health, Bethesda, MD, USA), with the RGB Color set to RGB Stack, and the contrast adjusted. The positive signal areas were selected and the % Area was calculated for the immunohistochemical positive area.

Cell culture and LPS treatment
C6 cells were purchased from Saibai Kang Biotechnology Co., Ltd. (Shanghai, China) and cultured in F12k medium with 15% horse serum, 2.5% FBS, 100 U/mL penicillin, and 100 U/mL streptomycin at 37 °C in a humidified atmosphere of 5% $CO_2$. When more than 80% of the cells were covered at the bottom of the culture flask, 0.25% trypsin was used to digest the cells for passage. The logarithmic growth period cells were adopted to carry out the experiment. Cells were treated with LPS (2 μg/mL) for 24 h.

Cell proliferation assay
The cells were digested with 0.25% trypsin and seeded into 96-well plates. Luteolin and LPS were added to the cells as indicated. After 48 h, the proliferation ability of the cells was tested following the instructions of the EDU kit (RIBBIO, Guangzhou, China).

NO testing
The fresh brain tissue of mice was diluted with normal saline to get 10% homogenate respectively and centrifuged at 4 °C at 2000 rpm for 10 min. The supernatant was collected from LPS-treated cells in the presence or absence of luteolin. NO content in homogenate and supernatant were then tested according to the instructions of NO kit (Nanjing Jiancheng Bioengineering Institute, Nanjing, China).

ELISA
The levels of TNF-α, IL-6, IL-1β in brain tissues and the supernatants were measured using ELISA Kits according to the manufacturer's instructions. Snap-frozen brains from treated mice were homogenized and lysed to perform ELISA from tissue lysate. Then, the absorbance of each well was obtained at 450 nm with a microplate reader.

Immunofluorescence double staining
Paraffin sections (5 μm) were deparaffinized and followed by citric acid buffer antigen repair and blocked with 5% BSA. Then the sections were incubated with anti-GRP78 and anti-GFAP primary antibodies at 4 °C overnight. After PBS wash, mixed second antibodies were applied for 1 h at room temperature, followed by PBS wash, DAPI (10 μg/mL) incubation in the dark for 10 min, and mounting. Images were taken by fluorescence microscope and the positive area rate was calculated by ImageJ 2.0, similar to the aforementioned immunohistochemical positive area.

Western blotting
Protein concentrations were measured using a protein assay kit according to the manufacturer's instructions. The extracted proteins were separated by SDS-polyacrylamide gel electrophoresis and then transferred to PVDF membranes for 30 min. The membranes were blocked with 5% skim milk for 2 h, and then incubated at 4 °C overnight with the following primary antibodies: anti-GRP78, anti-GFAP, anti-IRE1α, anti-NF-κB, anti-p-38, and anti-p-p38 respectively. The membrane was then washed with TBST three times and incubated with a second antibody (goat anti-mouse or goat anti-rabbit) for 2 h. Images were taken and analyzed with ImageJ 2.0.

Statistical analysis
Origin 8.0 was adopted for statistical analyses. All data were presented as mean ± SEM. Comparison among three groups was assessed by one-way ANOVA, followed by a least-significant difference test if normally distributed. Otherwise, Kruskal–Wallis test was utilized. $P < 0.05$ was considered statistically significant.

## RESULTS

Luteolin alleviates spatial learning deficits and brain histomorphology in model mice
In the Morris water maze test, all groups showed a certain learning ability during the 5-day training. The 3 × Tg-AD mice had a longer incubation period to reach the platform compared to the WT control group, and mice in the administration group had a shorter incubation period than 3 × Tg-AD mice (Fig. 1a, b).

When the test platform was hidden, the 3 × Tg-AD mice exhibited an aimless search strategy, while the mice receiving luteolin treatment spent a larger proportion of time in the target quadrant, and the number of times it crossed the platform position was similar to the WT control group (Fig. 1c–e).

Luteolin improves the brain histomorphology and reduces protein plaques in 3 × Tg-AD mice
To assess the effect of luteolin on the pathological changes in AD, histopathological changes and the number of dense Aβ plaques in the brain of 3 × Tg-AD mice were determined by Nissl's staining and Thioflavin S-staining, respectively. It was shown that luteolin improved the pathological deterioration of cerebral neurons in 3 × Tg-AD mice (Fig. 2a, b), and alleviated the cortical Aβ plaque burden in AD mice (Fig. 2c, d).

Luteolin inhibits over-activation of astrocytes in AD experimental animal and cell models
GFAP expression was detected in astrocytes from the cerebral cortex of mice with immunohistochemistry. Of note, GFAP expression is significantly higher in the cerebral cortex of 3 × Tg-AD mice than that of WT-Con mice, indicating an increase of reactive astrocytes in this model. In addition, luteolin reduced the expression of GFAP, suggesting a suppressive role of luteolin in the activation of astrocytes in the AD disease (Fig. 3a, b).

Next, we evaluated the effects of luteolin on cell viability in C6 cells. MTT results showed that luteolin ranging from 0 to 20 μmol/L had no obvious effect on the cell viability of C6 cells 24 h post-treatment. While suppressed C6 cell viability was exerted 48 h after luteolin treatment at the concentration of 10 μmol/L or even higher. The effects of luteolin on cell viability in C6 cells are shown in Supplementary Fig. S2a. High dose (10 μmol/L) and low dose (1 μmol/L) of luteolin were used to treat C6 cells in the presence or absence of LPS. It turned out C6 cells proliferated in LPS-induced inflammation, and displayed more inflammation reaction, and excessive activation of astrocytes with an increase in GFAP protein expression by Western blot. However, luteolin treatment could restore the cell proliferation and GFAP protein expression to a control level, indicating that luteolin inhibited the excessive activation of astrocytes (Fig. 3c–f).

Luteolin improves inflammation in AD experimental animal and cell models
Next, we measured the expression levels of inflammatory cytokines in 3 × Tg-AD mice. It was demonstrated that TNF-α, IL-1β, IL-6, NO, COX-2, and iNOS protein expression were significantly increased in 3 × Tg-AD mice, which could be restored in luteolin treated mice (Fig. 4a–c). Similar results were observed in LPS treated C6 cells (Fig. 4d–f). These results suggested that luteolin showed an inhibitory effect on neuroinflammation in both animal and cell models of AD.

Luteolin reduces the expression of ER stress-related proteins in AD experimental animal and cell models
To investigate the inhibitory mechanism of luteolin on ER stress, we detected two classic ER stress-related proteins in 3 × Tg-AD mice and C6 cells. Immunohistochemistry results showed that GRP78 and IRE1α were significantly increased in the brain tissues of 3 × Tg-AD mice, while luteolin treated mice exhibited lower expression of GRP78 and IRE1α compared to that of 3 × Tg-AD mice (Fig. 5a, b, d, e). In order to prove that the over-activation of astrocytes caused ER stress leading to neuroinflammation, we used immunofluorescence double-staining to detect the astrocytes marker GFAP and ER stress marker GRP78. It was shown that there was an increased expression and obvious co-localization of GFAP and GRP78 in brain tissues from 3 × Tg-AD mice, while luteolin reduced the expression and colocalization of these proteins (Fig. 5c, f). Moreover, the reduction

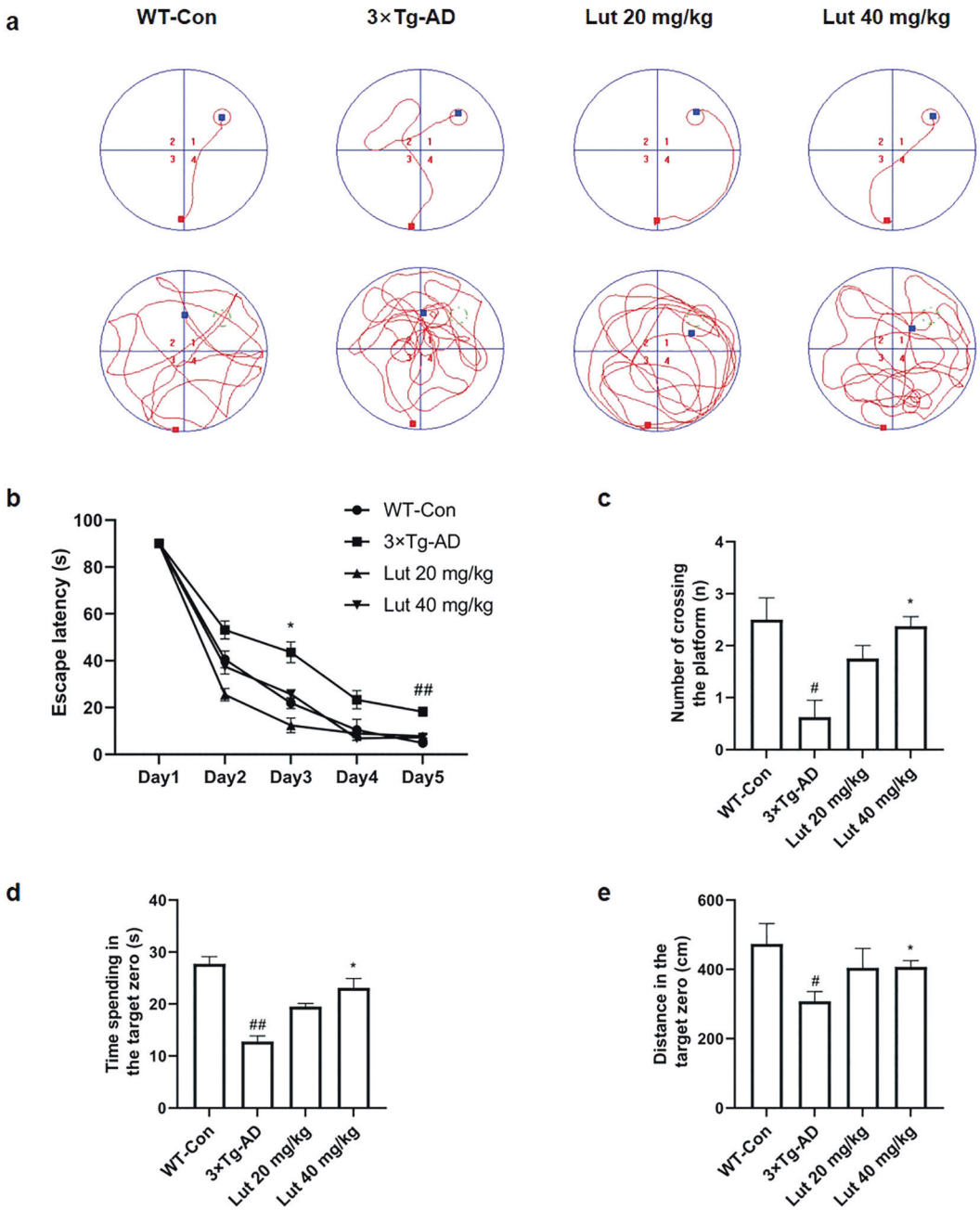


**Fig. 1 Luteolin ameliorated learning and memory impairment in 3 × Tg-AD mice.** The training trials were performed three times a day for 5 days. The swimming distance and swimming time before arrival at the platform were automatically recorded. Twenty-four hours after the training trials, a probe test was performed. **a** The tracks of the mice in the probe trial on the fifth day and without the platform. **b** Time to reach the hidden platform. **c** Number of times the mice crossed the platform location in the probe trial. **d** Spending time in the target zero. **e** Total swimming distance in the target zero. All values are presented as the means ± SEM, $n = 8$. $^{\#}P < 0.05$, $^{\#\#}P < 0.01$ versus WT-Con; $^{*}P < 0.05$ versus 3 × Tg-AD mice.

of GRP78 or IRE1α was unveiled in luteolin-treated C6 cells compared to control cells after LPS stimulation (Fig. 5g, h). It suggests that luteolin inhibited the ER stress signaling molecules in both the AD animal model and cell model.

Luteolin decreases the inflammatory signaling in AD experimental animal and cell models

In order to explore the inhibitory mechanism of luteolin on neuroinflammation, we detected two classical inflammatory signalings both in vivo and in vitro in the presence or absence of luteolin. The expression of p-NF-κB and phospho-p38 was significantly increased in the brain tissues of 3 × Tg-AD mice, while the expression of these proteins was decreased in luteolin treated mice (Fig. 6a–c). Similar results were also observed in LPS-treated C6 cells (Fig. 6d–f). It suggests that luteolin has inhibitory effects on classical inflammatory signaling molecules in both 3 × Tg-AD mice and LPS-treated C6 cells.

## DISCUSSION

AD is a progressive neurodegenerative disease characterized by cognitive impairment and behavioral changes caused by synaptic damage and neuron loss. Due to the complex pathological features and the unclear pathogenesis of AD, the clinical

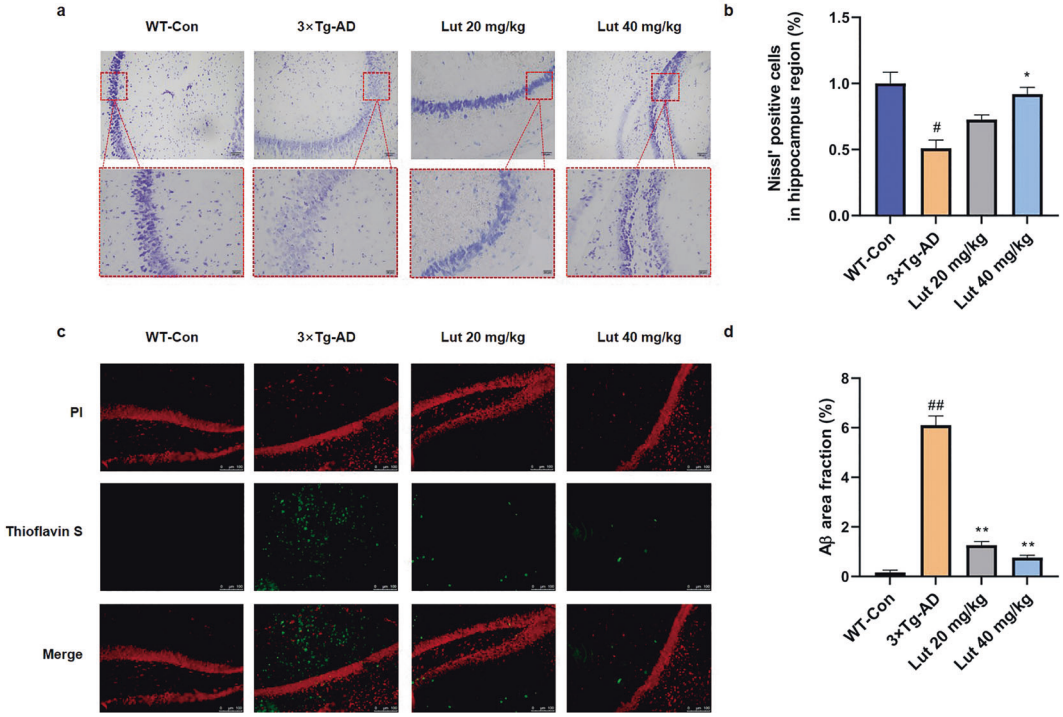


**Fig. 2 Luteolin improved the brain histomorphology and reduces protein plaques in 3 × Tg-AD mice. a** Nissl staining of the neuronal cells showed that Nissl substance was lost in neuronal cells in 3 × Tg-AD mice, while luteolin alleviated the pathological changes in neuronal cells. Representative images were chosen from each experimental group. Scale bar = 50 μm in original images and scale bar = 20 μm in enlarged plots. **b** Nissl staining positive cells (%) in the hippocampus. **c** Lutelion alleviated the cortical plaque burden in 3 × Tg-AD mice. Representative images were chosen from each experimental group. Scale bar = 100 μm. **d** Quantification of the surface area of Aβ plaques. All values are presented as the means ± SEM, $n = 3$. $^{\#}P < 0.05$, $^{\#\#}P < 0.01$ versus WT-Con; $^{*}P < 0.05$, $^{**}P < 0.01$ versus 3 × Tg-AD mice.

treatment is far from satisfactory and warrants further investigation [23, 24]. Flavonoid compounds derived from natural products have anti-inflammatory, antioxidant, antiviral, and other biological activities, and exert neuroprotective effects in many neurodegenerative disease models [25–27]. Luteolin, a flavonoid widely distributed in the plant kingdom, has antioxidant, anticancer, anti-inflammatory, and neuroprotective effects [28], but whether luteolin has therapeutic effects on AD remains unclear. To this end, 3 × Tg-AD mice were used as an AD model to investigate the effects of luteolin on learning and memory ability and pathological changes in mice [29]. Our study showed that luteolin significantly improved the learning and memory abilities of the 3 × Tg-AD mice, and the pathological examination showed that luteolin treatment reduced the loss of neurons and the burden of APs in the brain of the model mice.

Over the past few decades, it has been recognized that abnormal inflammatory processes in the CNS can lead to neurological dysfunction [30, 31]. Although inflammation is considered a beneficial physiological response because it promotes debris removal and tissue repair, while persistent inflammation eventually impairs neuronal function and leads to cell death [32, 33]. Our experimental results showed that there was a significant inflammatory response in the brain of the 3 × Tg-AD mice, and luteolin effectively inhibited the inflammatory response in the model mice. At the same time, luteolin also showed a significant inhibitory effect on LPS induced inflammatory response in C6 cells.

As a dominant resident cell population in the CNS, astrocytes are emerging as a research hotspot in neurodegenerative diseases such as AD in recent years. Astrocytes are involved in neurotransmitter uptake and circulation, inflammation, regulation of synaptic activity, ion balance and maintenance of the blood-brain barrier, etc [34–36]. They are important microenvironmental components for neurons to function well and the key is to maintain dynamic environmental balance in the brain. A growing body of evidence suggests that the pathogenesis of AD is not confined to the interneuron, but is closely related to glial cells in the brain [37]. Activation of glial cells may occur early in AD, even before Aβ deposition. Astrocyte pathological reaction is represented by astrocyte reactive hyperplasia. Reactive astrocyte is characterized by increased GFAP expression [38]. Intriguingly, our data showed a significantly increased GFAP expression, excessive activation, and proliferation of astrocytes in AD animal models, which could be retarded by luteolin treatment. This is also consistent with the inhibitory effect of luteolin on LPS induced neuroinflammation in C6 cells.

Under ER stress, cells escape severe damage by activating the adaptive response pathway of the UPR [39]. However, when ER stress persists, cells stop protecting themselves and are prone to cell death instead [40]. A large number of studies have reported upregulation of UPR-ER in the brain samples of patients with AD [41]. Therefore, the role of ER stress in AD cannot be ignored.

UPR-ER contains a complex network of three stress-reactive transmembrane proteins, such as RNA-like ER kinase (PERK), inositol enzyme 1 (IRE1), and activated transcription factor 6 (ATF6) [42–44]. In general, glucose-regulated protein 78 (GRP78) binds to these transmembrane proteins to maintain a stable, non-reactive state. When an injury causes ER stress, GRP78 is separated from them and activates the UPR response [45]. Therefore, GRP78 is considered an important marker of ER stress. In the mouse model of AD, activation of the ER stress response has also been reported. In line with the previous reports, we found that GRP78 expression increased in both 3 × Tg-AD mice and LPS-induced C6 cells, indicating that ER stress was present in both in vivo and in vitro models of AD, which could be ameliorated by luteolin in both conditions. To investigate the location of the ER stress response, we used immunofluorescence double-staining to label

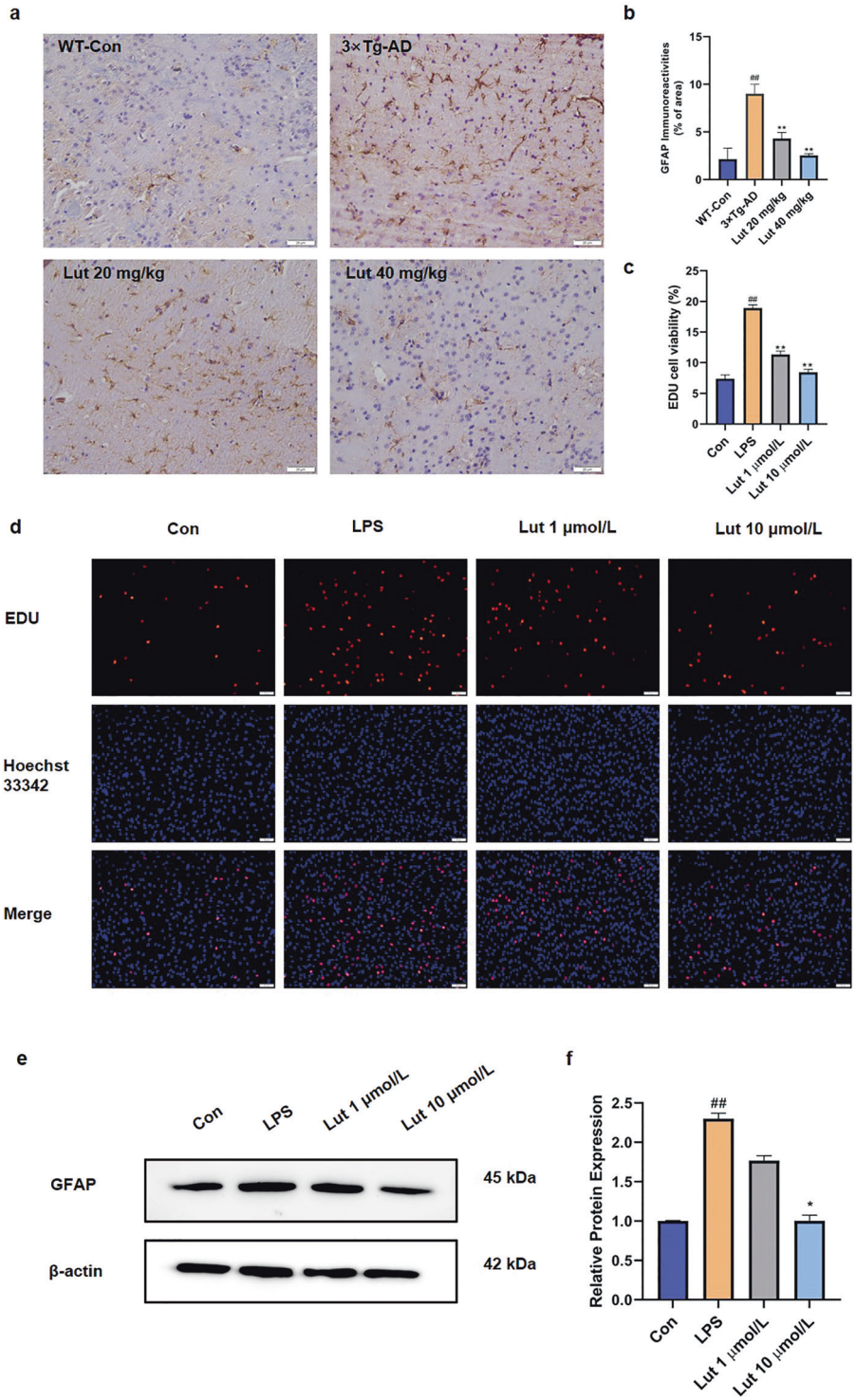


**Fig. 3 Luteolin inhibited overactivation of astrocytes in AD experimental and cell models. a** Immunohistochemical results showed that luteolin treatment reduced the expression of GFAP in the cerebral cortex of 3 × Tg-AD mice. The expression of GFAP increased significantly in 3 × Tg-AD mice, and a significant reduction was observed in luteolin treatment mice. **b** Quantification of average positive area. The data are expressed as the mean ± SEM, $n = 3$. $^{\#\#}P < 0.01$ versus WT-Con; $^{**}P < 0.01$ versus 3 × Tg-AD mice. **c** C6 cells had more proliferation post LPS treatment, while luteolin reduced the over-activation of C6 cells. **d** The quantification of cell viability. **e** The representative image and (**f**) quantification analysis showed GFAP expression was enhanced after the LPS challenge, which could be reduced by luteolin treatment. The data are expressed as the mean ± SEM, $n = 3$. $^{\#\#}P < 0.01$ versus control cells; $^{*}P < 0.05$, $^{**}P < 0.01$ versus LPS treated cells.

the astrocyte reactive protein GFAP and ER stress marker protein GRP78. It turned out that the co-localization of GFAP and GRP78 was obvious in 3 × Tg-AD mice, which indicated that ER stress occurred in astrocytes in the mouse brain.

During the ER stress response, PERK, IRE-1 triggers inflammatory signals. Among them, the adaptor protein TNF receptor-associated factor 2 (TRAF2) is recruited after IRE1α oligomeric reaction. The inflammatory pathway activated by the complexes includes the

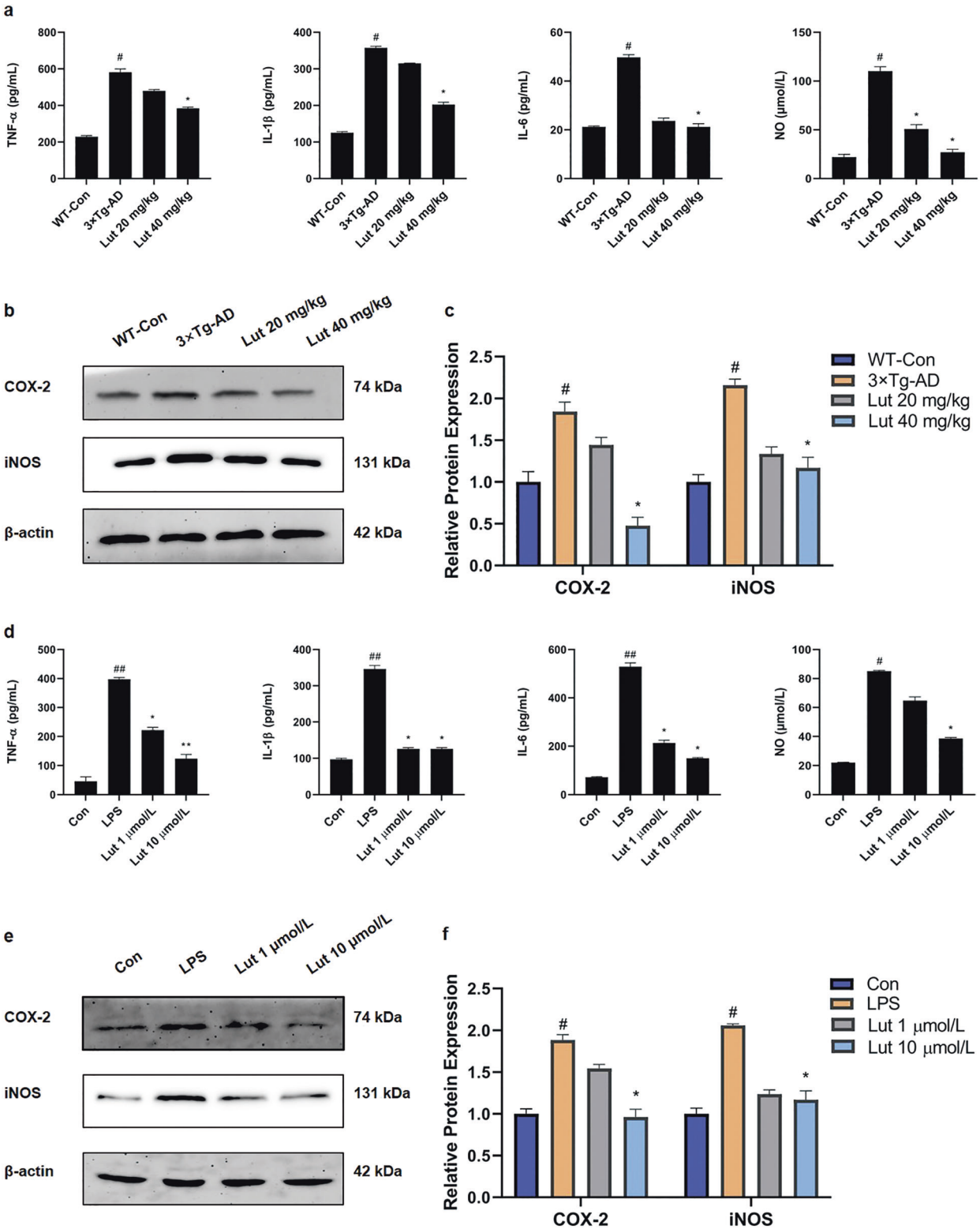


**Fig. 4 Luteolin reduced the level of inflammatory cytokines (TNF-α, IL-1β, IL-6, and NO) and the expression of COX-2 and iNOS both in 3 × Tg-AD mice and LPS-treated C6 cells. a** The inflammatory cytokines (TNF-α, IL-1β, IL-6, and NO) were higher in 3 × Tg-AD mice than WT-Con mice, and luteolin reduced the level of those inflammatory cytokines. **b** The representative images and (**c**) quantification analysis showed COX-2 and iNOS protein in 3 × Tg-AD mice was higher than WT control mice, which declined in luteolin treated 3 × Tg-AD mice. The data are expressed as the mean ± SEM, $n = 3$. $^{\#}P < 0.05$ versus WT-Con; $^{*}P < 0.05$ versus 3 × Tg-AD mice. **d** Luteolin decreased the level of inflammatory cytokines (TNF-α, IL-1β, IL-6, and NO) in LPS-induced C6 cells. **e** The representative images and (**f**) quantification showed COX-2 and iNOS protein was highly expressed in LPS-treated C6 cells than C6 cells, while luteolin decreased the expression of COX-2 and iNOS protein in LPS-induced C6 cells. The data are expressed as the mean ± SEM, $n = 3$. $^{\#}P < 0.05$, $^{\#\#}P < 0.01$ versus control cells; $^{*}P < 0.05$, $^{**}P < 0.01$ versus LPS treated cells.

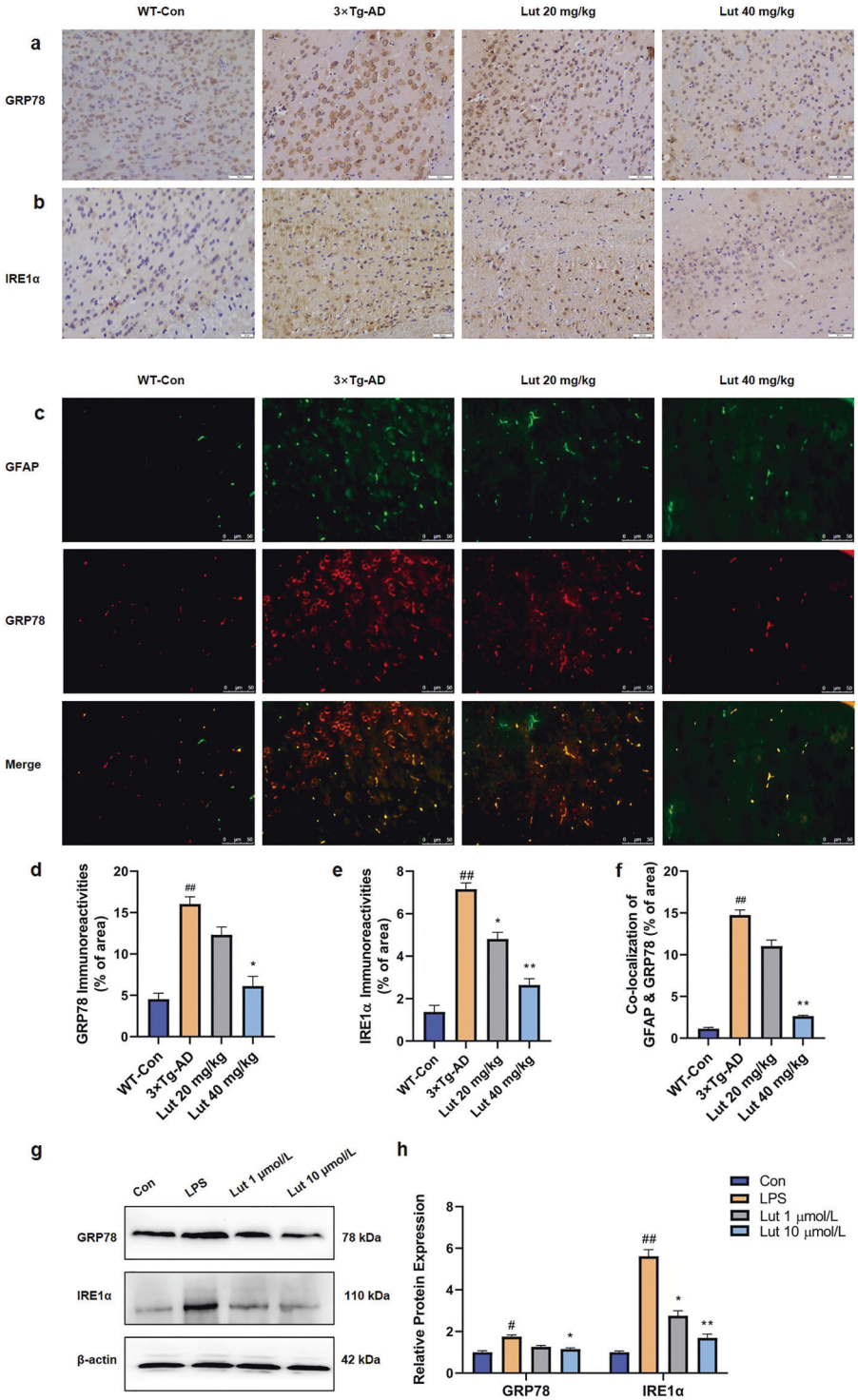


**Fig. 5 Luteolin reduced the expression of ER stress-related proteins in AD experimental animal and cell models, and luteolin reduced the expression and co-localization of GRP78 and GFAP in 3 × Tg-AD mice. a** Representative immunohistochemical images and (**d**) quantification analysis identified a higher proportion of GRP78$^{+}$ cells in 3 × Tg-AD mice, which could be restored after luteolin treatment. **b** Representative immunohistochemical images and (**e**) quantification analysis revealed luteolin reduced percentage of IRE1α$^{+}$ cells in 3 × Tg-AD mice. **c** Representative double staining fluorescent images and (**f**) quantification analysis showed a higher percentage of double-positive cells (GRP78$^{+}$ GFAP$^{+}$ cells) in 3 × Tg-AD mice could be limited by luteolin treatment. Scale bar = 50 μm. The data are expressed as the mean ± SEM, $n = 3$. $^{\#\#}P < 0.01$ versus WT-Con; $^{*}P < 0.05$, $^{**}P < 0.01$ versus 3 × Tg-AD mice. **g** Representative blotting bands and (**h**) quantification analysis showed luteolin reduced the expression of GRP78 and IRE1α in LPS-induced C6 cells. The data are expressed as the mean ± SEM, $n = 3$. $^{\#}P < 0.05$, $^{\#\#}P < 0.01$ versus control cells; $^{*}P < 0.05$, $^{**}P < 0.01$ versus LPS treated cells.

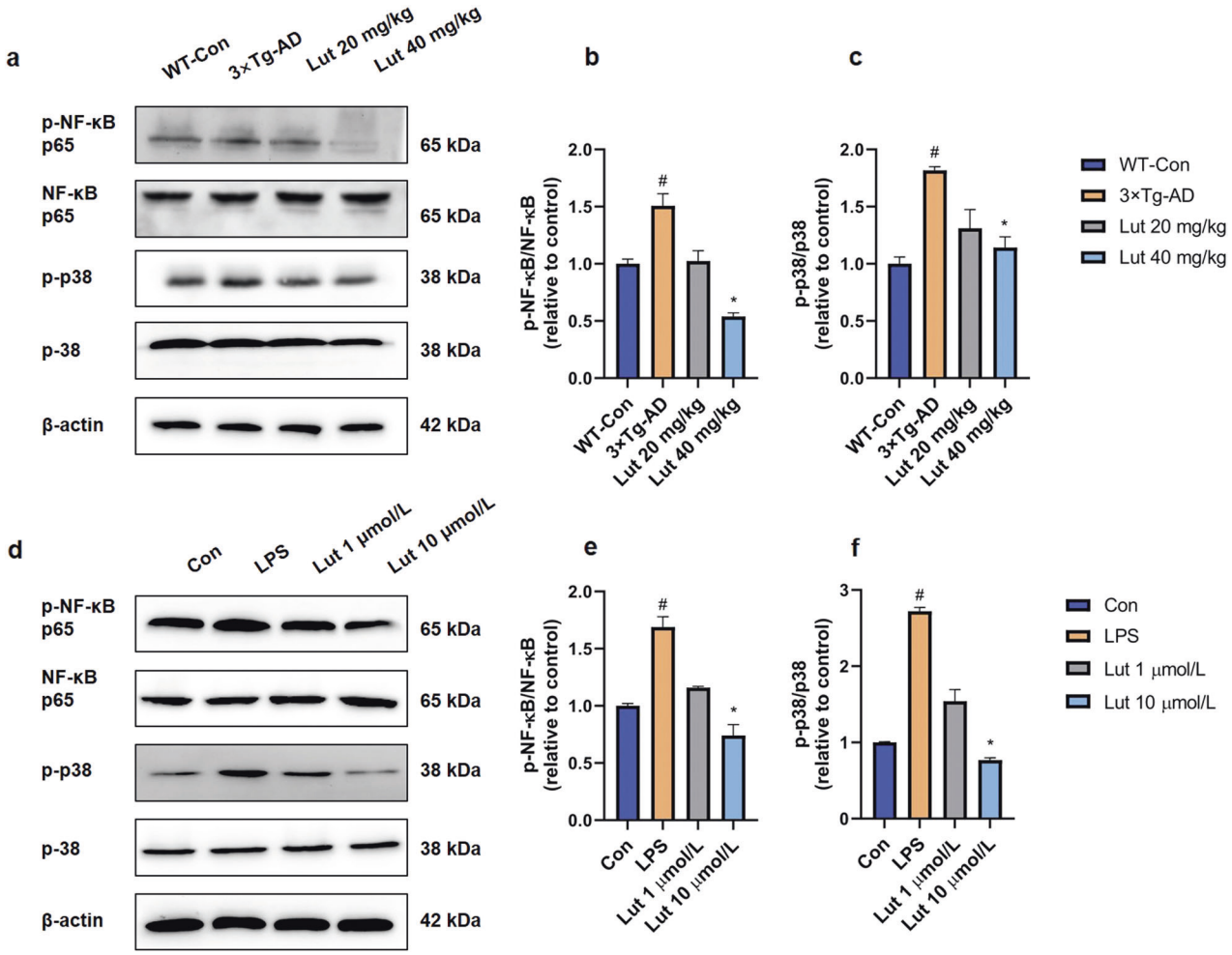


**Fig. 6 Luteolin decreased the inflammatory signaling in AD experimental and cell models. a** Representative Western blottings and (**b**), (**c**) quantification analysis showed p-NF-κB and p-p38 in 3 × Tg-AD mice was increased, and luteolin reduced the expression of p-NF-κB and p-p38. The data are expressed as the mean ± SEM, $n = 3$. $^{\#}P < 0.05$ versus WT-Con; $^{*}P < 0.05$ versus 3 × Tg-AD mice. **d** Representative images and (**e**), (**f**) quantification analysis demonstrated Luteolin reduced the expression of p-NF-κB and p-p38 in LPS-induced C6 cells. The data are expressed as the mean ± SEM, $n = 3$. $^{\#}P < 0.05$ versus control cells; $^{*}P < 0.05$ versus LPS treated cells.

nuclear transcription factor Kappa-light-chain-enhancer activated B cells (NF-κB) and the proteins of the MAPK family c-Jun N-terminal kinase (JNK) and P38 [46, 47]. To investigate the relationship between neuroinflammation and ER stress in AD, expression of IRE1α and p-NF-κB, NF-κB, p38, and p-p38 were also measured. Notably, 3 × Tg-AD mice and the LPS-treated C6 cells have higher expression of IRE1α, p-NF-κB, and p-p38. These results suggest that ER stress occurs in animal and cell models of AD, and mediates the activation of NF-κB and p38 inflammatory pathways probably through the IRE1α-TRAF2 axis, then leads to neuroinflammation. Luteolin was proved to exert a suppressive role against ER stress activation and inflammatory signaling pathways in AD animal and cell models.

## CONCLUSION

Astrocyte plays an important role of maintaining the function of the nervous system. The occurrence of AD may be due to ER stress of astrocytes, which leads to the occurrence of the inflammatory response, resulting in loss of neuronal synapses, neurological dysfunction, and reduction of learning and memory ability. Luteolin inhibited the aggravation of neuroinflammation by inhibiting ER stress in 3 × Tg-AD mice, thus relieving the learning and memory impairment in mice (Fig. 7).

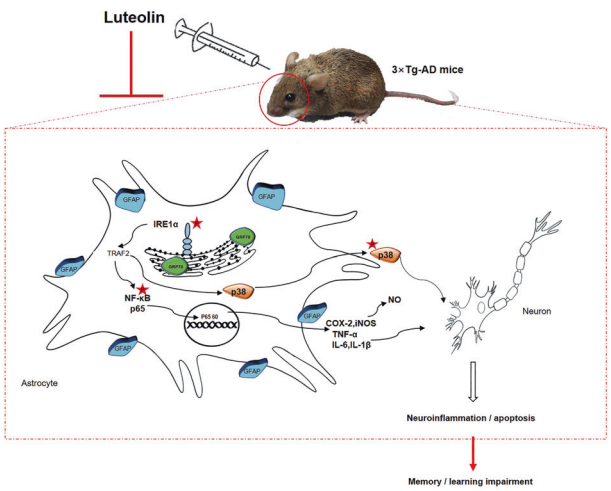


**Fig. 7 The mechanism of luteolin alleviating cognitive impairment in 3 × Tg-AD mice.** Luteolin inhibits the activation of NF-κB and p38 inflammatory pathways mediated by ER stress, then reduces the level of inflammatory cytokine, the expression of COX-2 and iNOS, and eventually improves the learning and memory ability of 3 × Tg-AD mice.

## ACKNOWLEDGEMENTS

This study was supported by grants from the National Natural Science Foundation of China (No. 31872311), and the Science Foundation for Outstanding Young Scholars of Henan Province (No. 212300410027).

## AUTHOR CONTRIBUTIONS

JJK, JZS, and YYH designed the study and performed and interpreted the data of mice and cell experiments. JJK, JZS, YYH, JJH, HYZ, and DML performed the Morris water maze. JKS and XBP participated in the study design. XMX, JJK, and YY wrote the manuscript. XBP and GHD conceived and supervised the study, and revised the manuscript.

## ADDITIONAL INFORMATION

**Supplementary information** The online version contains supplementary material available at https://doi.org/10.1038/s41401-021-00702-8.

**Conflict of interest:** The authors declare no competing interests.

## REFERENCES

1. Hannah JA. A case of Alzheimer's disease with neuropathological findings. Can Med Assoc J. 1936;35:361–6.
2. Jahn H. Memory loss in Alzheimer's disease. Dialogues Clin Neurosci. 2013;15:445–54.
3. Alzheimer's Association. 2016 Alzheimer's disease facts and figures. Alzheimers Dement. 2016;12:459–509.
4. Glenner GG. Amyloid beta protein and the basis for Alzheimer's disease. Prog Clin Biol Res. 1989;317:857–68.
5. Shin RW, Iwaki T, Kitamoto T, Sato Y, Tateishi J. Massive accumulation of modified tau and severe depletion of normal tau characterize the cerebral cortex and white matter of Alzheimer's disease. Demonstration using the hydrated autoclaving method. Am J Pathol. 1992;140:937–45.
6. Zhang F, Zhong RJ, Cheng C, Li S, Le WD. New therapeutics beyond amyloid-β and tau for the treatment of Alzheimer's disease. Acta Pharmacol Sin. 2020 https://doi.org/10.1038/s41401-020-00565-5.
7. Zhu S, Wang J, Zhang Y, He J, Kong J, Wang JF, et al. The role of neuroinflammation and amyloid in cognitive impairment in an APP/PS1 transgenic mouse model of Alzheimer's disease. CNS Neurosci Ther. 2017;23:310–20.
8. Hauss-Wegrzyniak B, Dobrzanski P, Stoehr JD, Wenk GL. Chronic neuroinflammation in rats reproduces components of the neurobiology of Alzheimer's disease. Brain Res. 1998;780:294–303.
9. Cai Z, Hussain MD, Yan LJ. Microglia, neuroinflammation, and beta-amyloid protein in Alzheimer's disease. Int J Neurosci. 2014;124:307–21.
10. Altstiel LD, Sperber K. Cytokines in Alzheimer's disease. Prog Neuropsychopharmacol Biol Psychiatry. 1991;15:481–95.
11. Rehman SU, Ali T, Alam SI, Ullah R, Zeb A, Lee KW, et al. Ferulic acid rescues LPS-induced neurotoxicity via modulation of the TLR4 receptor in the mouse hippocampus. Mol Neurobiol. 2019;56:2774–90.
12. Guillamón-Vivancos T, Gómez-Pinedo U, Matías-Guiu J. Astrocytes in neurodegenerative diseases (I): function and molecular description. Neurologia. 2015;30:119–29.
13. Zhang F, Zhang JG, Yang W, Xu P, Xiao YL, Zhang HT. 6-Gingerol attenuates LPS-induced neuroinflammation and cognitive impairment partially via suppressing astrocyte overactivation. Biomed Pharmacother. 2018;107:1523–9.
14. Liu MQ, Chen Z, Chen LX. Endoplasmic reticulum stress: a novel mechanism and therapeutic target for cardiovascular diseases. Acta Pharmacol Sin. 2016;37:425–43.
15. Mattson MP, Guo Q, Furukawa K, Pedersen WA. Presenilins, the endoplasmic reticulum, and neuronal apoptosis in Alzheimer's disease. J Neurochem. 1998;70:1–14.
16. Hoozemans JJ, Veerhuis R, Van Haastert ES, Rozemuller JM, Baas F, Eikelenboom P, et al. The unfolded protein response is activated in Alzheimer's disease. Acta Neuropathol. 2005;110:165–72.
17. Costa RO, Ferreiro E, Martins I, Santana I, Cardoso SM, Oliveira CR, et al. Amyloid β-induced ER stress is enhanced under mitochondrial dysfunction conditions. Neurobiol Aging. 2012;33:824.e5–16.
18. Aziz N, Kim MY, Cho JY. Anti-inflammatory effects of luteolin: a review of in vitro, in vivo, and in silico studies. J Ethnopharmacol. 2018;225:342–58.
19. Nabavi SF, Braidy N, Gortzi O, Sobarzo-Sanchez E, Daglia M, Skalicka-Woźniak K, et al. Luteolin as an anti-inflammatory and neuroprotective agent: a brief review. Brain Res Bull. 2015;119:1–11. Pt A
20. Oddo S, Caccamo A, Shepherd JD, Murphy MP, Golde TE, Kayed R, et al. Triple-transgenic model of Alzheimer's disease with plaques and tangles: intracellular Abeta and synaptic dysfunction. Neuron. 2003;39:409–21.
21. Xiong J, Wang K, Yuan C, Xing R, Ni J, Hu G, et al. Luteolin protects mice from severe acute pancreatitis by exerting HO-1-mediated anti-inflammatory and antioxidant effects. Int J Mol Med. 2017;39:113–25.
22. Kou J, Wang M, Shi J, Zhang H, Pu X, Song S, et al. Curcumin reduces cognitive deficits by inhibiting neuroinflammation through the endoplasmic reticulum stress pathway in apolipoprotein E4 transgenic mice. ACS Omega 2021;6:6654–62.
23. Gao LB, Yu XF, Chen Q, Zhou D. Alzheimer's disease therapeutics: current and future therapies. Minerva Med 2016;107:108–13.
24. Briggs R, Kennelly SP, O'Neill D. Drug treatments in Alzheimer's disease. Clin Med. 2016;16:247–53.
25. Maleki SJ, Crespo JF, Cabanillas B. Anti-inflammatory effects of flavonoids. Food Chem. 2019;299:125124.
26. Spagnuolo C, Moccia S, Russo GL. Anti-inflammatory effects of flavonoids in neurodegenerative disorders. Eur J Med Chem. 2018;153:105–15.
27. Li Q, Tian Z, Wang M, Kou J, Wang C, Rong X, et al. Luteoloside attenuates neuroinflammation in focal cerebral ischemia in rats via regulation of the PPARγ/Nrf2/NF-κB signaling pathway. Int Immunopharmacol. 2019;66:309–16.
28. Kempuraj D, Thangavel R, Kempuraj DD, Ahmed ME, Selvakumar GP, Raikwar SP, et al. Neuroprotective effects of flavone luteolin in neuroinflammation and neurotrauma. Biofactors. 2021;47:190–7.
29. Chen Y, Liang Z, Blanchard J, Dai CL, Sun S, Lee MH, et al. A non-transgenic mouse model (icv-STZ mouse) of Alzheimer's disease: similarities to and differences from the transgenic model (3xTg-AD mouse). Mol Neurobiol. 2013;47:711–25.
30. Thonhoff JR, Simpson EP, Appel SH. Neuroinflammatory mechanisms in amyotrophic lateral sclerosis pathogenesis. Curr Opin Neurol. 2018;31:635–9.
31. Thummayot S, Tocharus C, Jumnongprakhon P, Suksamrarn A, Tocharus J. Cyanidin attenuates $A\beta_{25\text{-}35}$-induced neuroinflammation by suppressing NF-κB activity downstream of TLR4/NOX4 in human neuroblastoma cells. Acta Pharmacol Sin. 2018;39:1439–52.
32. Glass CK, Saijo K, Winner B, Marchetto MC, Gage FH. Mechanisms underlying inflammation in neurodegeneration. Cell. 2010;140:918–34.
33. Akiyama H. Inflammatory response in Alzheimer's disease. Tohoku J Exp Med. 1994;174:295–303.
34. Acosta C, Anderson HD, Anderson CM. Astrocyte dysfunction in Alzheimer disease. J Neurosci Res. 2017;95:2430–47.
35. Sofroniew MV. Astrocyte barriers to neurotoxic inflammation. Nat Rev Neurosci. 2015;16:249–63.
36. Verkhratsky A, Nedergaard M. Physiology of astroglia. Physiol Rev. 2018;98:239–389.
37. Fakhoury M. Microglia and astrocytes in Alzheimer's disease: implications for therapy. Curr Neuropharmacol. 2018;16:508–18.
38. Phatnani H, Maniatis T. Astrocytes in neurodegenerative disease. Cold Spring Harb Perspect Biol. 2015;7:a020628.
39. Schröder M, Kaufman RJ. ER stress and the unfolded protein response. Mutat Res. 2005;569:29–63.
40. Sano R, Reed JC. ER stress-induced cell death mechanisms. Biochim Biophys Acta. 2013;1833:3460–70.
41. Scheper W, Hoozemans JJ. The unfolded protein response in neurodegenerative diseases: a neuropathological perspective. Acta Neuropathol. 2015;130:315–31.
42. Schröder M, Kaufman RJ. The mammalian unfolded protein response. Annu Rev Biochem. 2005;74:739–89.
43. Richie DL, Hartl L, Aimanianda V, Winters MS, Fuller KK, Miley MD, et al. A role for the unfolded protein response (UPR) in virulence and antifungal susceptibility in Aspergillus fumigatus. PLoS Pathog. 2009;5:e1000258.
44. Rahman S, Archana A, Jan AT, Minakshi R. Dissecting endoplasmic reticulum unfolded protein response (UPRER) in managing clandestine modus operandi of Alzheimer's disease. Front Aging Neurosci. 2018;10:30.
45. Walter P, Ron D. The unfolded protein response: from stress pathway to homeostatic regulation. Science. 2011;334:1081–6.
46. Pahl HL, Baeuerle PA. A novel signal transduction pathway from the endoplasmic reticulum to the nucleus is mediated by transcription factor NF-kappa B. EMBO J. 1995;14:2580–8.
47. Wang YL, Zhou X, Li DL, Ye JM. Role of the mTOR-autophagy-ER stress pathway in high fructose-induced metabolic-associated fatty liver disease. Acta Pharmacol Sin. 2021. https://doi.org/10.1038/s41401-021-00629-0.